3D analysis of losses in the shields of SC coils in EDS-MAGLEV transport systems

M. Andriollo, G. Martinelli, A. Morini & A. Scuttari
Department of Electrical Engineering, University of Padova, Via Gradenigo 6/a, I-35131 Padova, Italy

Abstract

The paper firstly describes a 3D analytical method to calculate the currents in the on-ground levitation coils of an EDS-MAGLEV train; such currents are then used as inputs for a 3D FEM code to calculate the eddy currents and losses in the shields of the on-board SC coils.

1 Introduction

The suspension of magnetically levitated trains of electrodynamic type (EDS-MAGLEV) is due to the repulsive force between on-board superconducting (SC) magnets and the reaction field produced by currents dynamically induced in on-ground levitation coils. The SC magnets also provide the excitation field of the linear synchronous motor which propels the train; the armature winding of the motor is placed along the guideway [1].
An important technical point is the design of the shields which protect the SC coils. Such design needs the verification of losses and forces due to the eddy currents in the shields, as both over-heating and mechanical vibrations may cause the quenching of the SC wires. Eddy currents are induced in the shields by both non-synchronous components of the armature field and the reaction field produced by the levitation coils [2].

The paper deals with the determination of the reaction field and the resulting distribution of eddy currents in the shields. The analysis of such phenomena is difficult, as the currents in the levitation coils are not sinusoidal [3,4], and then the determination of the reaction field needs a harmonic analysis. Furthermore, the e.m.f.s induced in the shields have also dynamical components, due to the relative motion between train and ground. To-day, the most widely spread FEM commercial packages don't allow 3D analysis of magnetic field

taking into account both the harmonic spectrum of source currents and the presence of eddy currents of dynamical origin.

The proposed method consists of the following points:

- with reference to a 3D analytical method [3,4], the time harmonics of the current induced in the generic levitation coil are evaluated;
- summing up the effects of all the coils, the spatial harmonics of the resulting current density with respect to the vehicle are determined;
- for each harmonic, suitable analytical functions are considered to approximate the calculated distribution: such functions are the inputs for 3D FEM analysis;
- with reference to a generic shield, the eddy current density and resultant losses are determined.

In the example of application some results are given.

2 Configuration

The considered train car carries eight SC coils, four (two per side) per end; the end coils of a car are assembled with the ones of the contiguous car to form a bogie [1]. As far as the levitation coils are concerned, the configuration with 8-shaped coils is considered [1], in which each on-ground levitation coil is composed of two unit coils connected to form an 8-shaped coil (Fig.1). Anyway, the developed analytical formulations can be applied to other and more general coil configurations.

The following hypotheses are assumed:

- the coils are rectangular;
- the current in the SC coils is constant;
- the currents induced in the levitation coils are calculated taking into account the effect of the excitation field only (it has been verified that the shield eddy currents practically don't modify the field component perpendicular to the plane of levitation coils and then the impressed currents);
- a steady-state running at speed υ is considered.

3 Current density in the levitation coils (analytical method)

Given a reference system (x,y,z) fixed to the vehicle and with origin in the centre of the first SC coil in the motion direction, the current induced in the k-th (k=1,2,...,N) levitation coil is given by [3,4,5]:

$$i_t^{(k)}(t) = \frac{M_0 I_S}{L-M} \sum_{n=1}^{\infty} \frac{nS_n^* Q''}{\sqrt{1+(n\lambda_n'' Q'')^2}} \cos\left\{nq_y\left[Y_0 - \upsilon t + (k-1)p\right] + \varphi_n\right\} \qquad (1)$$

The expressions of M_0, S^*_n Q'' and φ_n are given in Appendix; λ''_n is a coefficient which takes into account the mutual coupling between all the levitation coils of the row [3,4].

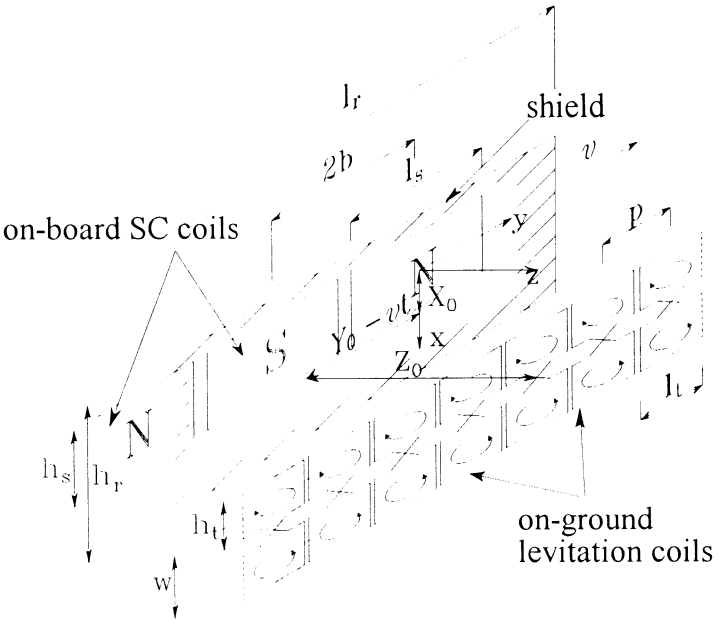

Figure 1: *Arrangement of coils and shield with reference to one side of the train and guideway (for the sake of clearness the coils are represented as filiform and the armature coils are not represented).*

The spatial distribution of the components of the current density related to the k-th levitation coil can be represented by means of a double Fourier series expansion along y and x. The obtained relations are:

$$G_x^{(k)}(x,y,t) = -2\sum_{n=1}^{\infty}\sum_{\substack{m=2\ell+1\\ \ell=0,1,2,\ldots}}^{\infty} G_{xnm}^{(k)} \sin\left(mq_x\frac{w}{2}\right)\sin\left[mq_x(x-X_0)\right]\cdot \cdot\sin\left[nq_y(y-Y_0+\upsilon t-kp)\right] \tag{3}$$

$$G_y^{(k)}(x,y,t) = 2\sum_{n=0}^{\infty}\sum_{\substack{m=2\ell+1\\ \ell=0,1,2,\ldots}}^{\infty} G_{ynm}^{(k)} \sin\left(mq_x\frac{w}{2}\right)\cos\left[mq_x(x-X_0)\right]\cdot \cdot\cos\left[nq_y(y-Y_0+\upsilon t-kp)\right] \tag{4}$$

with:

$$G_{xnm}^{(k)} = -\frac{8N_t i_t^{(k)}}{\pi^2 m s_t t_t}\cdot\Gamma_{nm}(l_t,h_t,t_t) \tag{5}$$

$$G_{ynm}^{(k)} = -\frac{mq_x}{nq_y} G_{xnm}^{(k)} \quad (n\neq 0) \qquad G_{y0m}^{(k)} = \frac{4N_t i_t^{(k)}}{\pi^2 m s_t t_t} \cdot \Gamma_{0m}(l_t, h_t, t_t) \quad (n=0) \quad (6)$$

The expressions of $\Gamma_{nm}(l,h,t)$ and $\Gamma_{0m}(l,h,t)$ are given in Appendix.

The superposition of effects of N levitation coils lets eqns (3) and (4) be substituted by:

$$G_x(x,y,t) = \sum_{k=1}^{N} G_x^{(k)}(x,y,t) \quad (7)$$

$$G_y(x,y,t) = \sum_{k=1}^{N} G_y^{(k)}(x,y,t) \quad (8)$$

Bearing in mind eqns (1), (5) and (6) and pointing out the time dependence, eqns (7) and (8) may be written in the following way ($\omega=q_y\upsilon$):

$$G_x(x,y,t) = N\left\{\sum_{i=1}^{\infty}\left[G_{x,iN}^{(c)}(x,y)\cos(iN\omega t) + G_{x,iN}^{(s)}(x,y)\sin(iN\omega t)\right]\right\} \quad (9)$$

$$G_y(x,y,t) = N\left\{\sum_{i=0}^{\infty}\left[G_{y,iN}^{(c)}(x,y)\cos(iN\omega t) + G_{y,iN}^{(s)}(x,y)\sin(iN\omega t)\right]\right\} \quad (10)$$

The coefficients $G^{(c)}_{x,iN}$, $G^{(s)}_{x,iN}$, $G^{(c)}_{y,iN}$ and $G^{(s)}_{y,iN}$ are functions of x and y and are expressible as Fourier series expansions (see Appendix). It must be pointed out that only terms with harmonic order N and multiple are present.

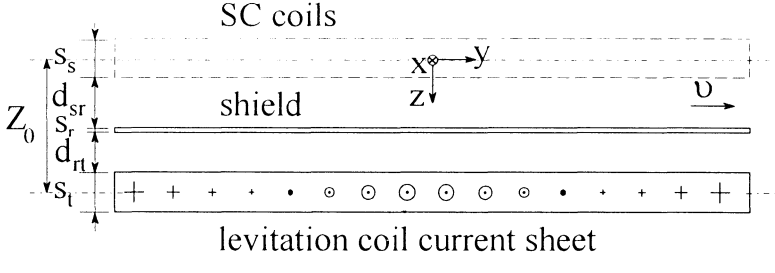

Figure 2: Cross section of coils and shield.

4 Eddy currents and losses in the shield (numerical method)

In order to take into account the influence of the shield, 3D FEM numerical code (ANSOFT Maxwell Field Solver) has been utilized.

Assuming that only speed y-component is present and relating to a reference system fixed to the ground, the following vectorial time-varying equation is valid:

$$\nabla^2 \mathbf{A}_t = -\mu_0 \mathbf{G}_t + \mu\sigma \frac{\partial \mathbf{A}_t}{\partial t} + \upsilon\mu\sigma \frac{\partial \mathbf{A}_t}{\partial y} \tag{11}$$

with $\mathbf{A}_t$ vector potential related to the current density $\mathbf{G}_t$ in the levitation coils. Three regions are present, in which eqn (11) is particularized (Fig.2):

- inside levitation coils. Neglecting stray currents in levitation coils and assuming therefore current density $\mathbf{G}_t$ as impressed, eqn (11) becomes:

$$\nabla^2 \mathbf{A}_t = -\mu_0 \mathbf{G}_t \tag{12}$$

- inside levitation coils The impressed current is null and then:

$$\nabla^2 \mathbf{A}_t = \mu_0 \sigma \frac{\partial \mathbf{A}_t}{\partial t} + \upsilon \mu_0 \sigma \frac{\partial \mathbf{A}_t}{\partial y} \tag{13}$$

- outside levitation coils and shield. Impressed current as well as time- and motion- depending terms are null. This is valid inside the SC coils too: the excitation field is fixed with respect to the shield and then the SC coils do not cause eddy currents in the shield. Eqn (11) becomes the Laplace equation:

$$\nabla^2 \mathbf{A}_t = 0 \tag{14}$$

The utilized FEM code does not allow to take into account the dynamical effect due to relative motion between the field source and the material where eddy currents flow: the dynamical term of eqn (13) cannot be taken into account. Furthermore, the eddy-current module works in sinusoidal conditions, turning the problem of solving eqns (12)÷(14) into the problem of solving the corresponding complex equations. Nevertheless, according to eqns (9) and (10), the analysis is equivalent to the superposition of effects of sinusoidal distributions fixed to the vehicle with amplitude depending on x and y, and with angular frequency iNω. In this way, the dynamical term in eqn (13) disappears and the FEM analysis is possible, considering the harmonic components separately. The integration of the following complex equations is then required:

- inside levitation coils $(Z_0 - \frac{s_t}{2} \le z \le Z_0 + \frac{s_t}{2})$:
$$\nabla^2 \overline{\mathbf{A}}_{it}^{(c)} = -\mu\, \overline{\mathbf{G}}_{it}^{(c)}$$
$$\nabla^2 \overline{\mathbf{A}}_{it}^{(s)} = -\mu\, \overline{\mathbf{G}}_{it}^{(s)}$$

- inside levitation coils $(d_{sr} + \frac{s_s}{2} - \frac{s_r}{2} \le z \le d_{sr} + \frac{s_s}{2} + \frac{s_r}{2})$:
$$\nabla^2 \overline{\mathbf{A}}_{it}^{(c)} = j\mu\sigma \overline{\mathbf{A}}_{it}^{(c)}$$
$$\nabla^2 \overline{\mathbf{A}}_{it}^{(s)} = j\mu\sigma \overline{\mathbf{A}}_{it}^{(s)}$$

- in the other regions:
$$\nabla^2 \overline{\mathbf{A}}_{it}^{(c)} = 0$$
$$\nabla^2 \overline{\mathbf{A}}_{it}^{(s)} = 0$$

$\overline{\mathbf{A}}_{it}^{(c)}$, $\overline{\mathbf{G}}_{it}^{(c)}$ are phasors corresponding to the cosine component of vectors $\mathbf{A}_t$ and $\mathbf{G}_t$ with angular frequency iNω; similarly $\overline{\mathbf{A}}_{it}^{(s)}$ and $\overline{\mathbf{G}}_{it}^{(s)}$ correspond to the sine component. Once suitable boundary conditions have been imposed, the flux

density components $\overline{\mathbf{B}}_{ir}^{(c)}$ and $\overline{\mathbf{B}}_{ir}^{(s)}$ can be calculated; the determination of the components $\overline{\mathbf{G}}_{ir}^{(c)}$ and $\overline{\mathbf{G}}_{ir}^{(s)}$ of the shield current density $\mathbf{G}_r$ follows.

Finally, the total mean specific losses in the shield are given by:

$$< p_r >= \sum_{i=1}^{\infty} < p_{ir} > = \sum_{i=1}^{\infty} \frac{1}{\sigma} \left(\overline{\mathbf{G}}_{ir}^{(c)} + \overline{\mathbf{G}}_{ir}^{(s)} \right) \cdot \left(\overline{\overline{\mathbf{G}}}_{ir}^{(c)} + \overline{\overline{\mathbf{G}}}_{ir}^{(s)} \right) \tag{15}$$

where $<p_{ir}>$ are the losses due to the iN-th harmonic and $\overline{\overline{\mathbf{G}}}_{ir}^{(c)}$, $\overline{\overline{\mathbf{G}}}_{ir}^{(s)}$ the complex conjugate of the harmonic components of the shield current density.

5 Example of application

With reference to the data of Tab.1 (partially from [1] and [2]) and according to eqns (9) and (10), the harmonic components iN=48, 96 and 144 of the current density in the levitation coils have been evaluated.

Table I: *Parameters related to the configuration of Figs.1 and 2.*

l_s=1.020 m	h_s=0.450 m	s_s=0.080 m	t_s=0.050 m
N_s=1000	I_s=700 A	a_y=0.230 m	b_y=21.6 m
l_r=5.500 m	h_r=0.650 m	s_r=0.004 m	d_{rt}=0.100 m
σ=3.33·10^7 S/m	l_t=0.265 m	h_t=0.255 m	s_t=0.030 m
t_t=0.085 m	N_t=1	R=16.5 μΩ	L=0.518 μH
M=−0.036 μH	w=0.430 m	N=48	g_x=3.5 m
X_0=−0.035 m	Y_0=0.0 m	Z_0=0.185 m	υ=500 km/h

Fig.3 gives the amplitudes $G^{(c)}_{x,iN}(x,y)$ and $G^{(s)}_{x,iN}(x,y)$, calculated along y in correspondence of the centre of upper unit coils (x=−0.18 m). Similarly, Fig.4 gives he components $G^{(c)}_{y,iN}$ and $G^{(s)}_{y,iN}$ along y in correspondence of the upper end-zone of the lower unit coils (x=−0.005 m). The diagrams show oscillations with a mean period along y inversely proportional to the time frequency of the related harmonic. For the fundamental (iN=48) this period is $2\tau \cong 0.54$ m, for the second harmonic is $2\tau/2 \cong 0.27$ m, and so on. Furthermore, the displacement along y of the sine and cosine amplitudes of the generic i-th harmonic is about $\tau/2i$ (1/4 of period.). The space and time displacements of the sine and cosine components of the generic harmonic result in a wave travelling at speed $2N\upsilon\tau/b_y \cong 167$ m/s.with respect to the train. The amplitudes of the first three harmonics are of the same quantity. A sensible amplitude reduction is found only starting from the fourth harmonic (iN=192). With reference to the eddy-current losses in the shield, it is difficult to evaluate in advance what harmonic causes the main contribution, as the losses depend on the levitation coil current as well as on the harmonic frequency and period along y.

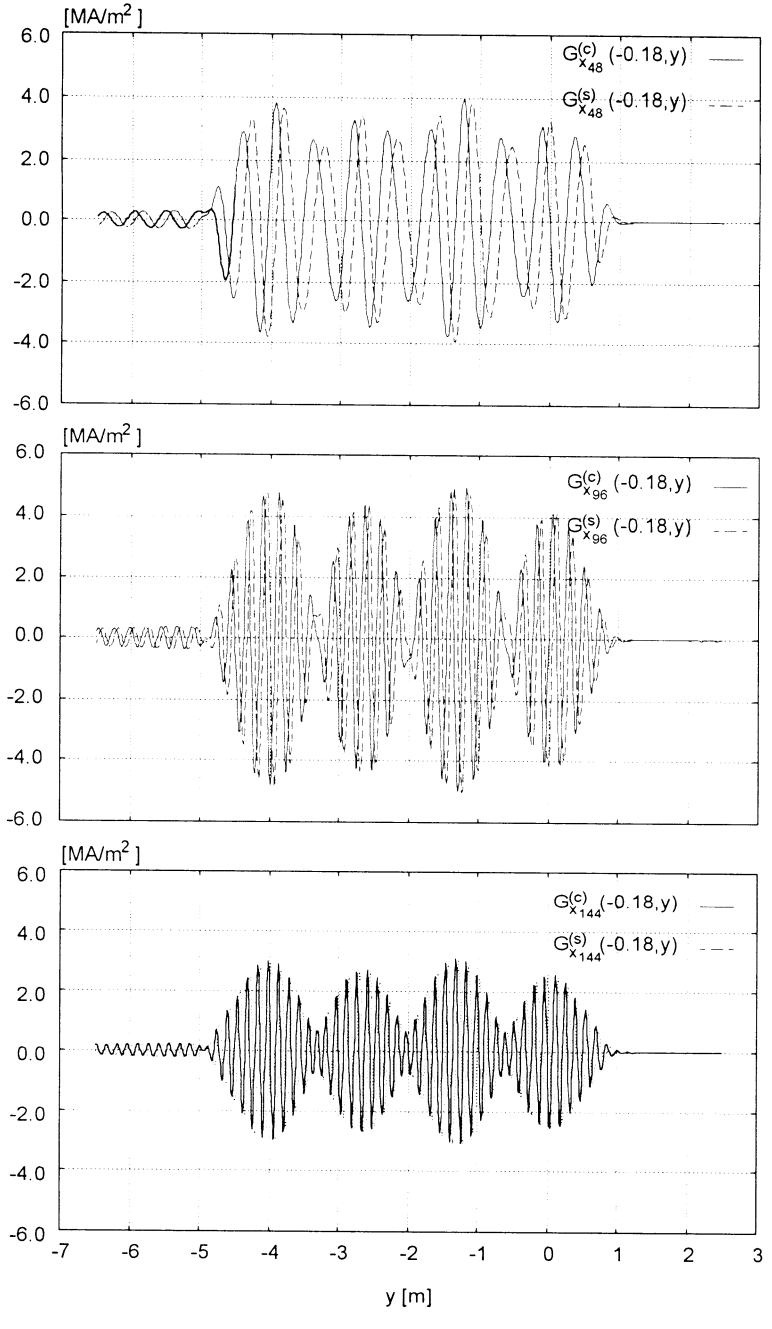

Figure 3: *Current density in the levitation coils: amplitudes of cosine and sine terms of the 1st, 2nd and 3rd harmonic (iN=48, 96, 144) of the x-component along y at x=–0.18 m.*

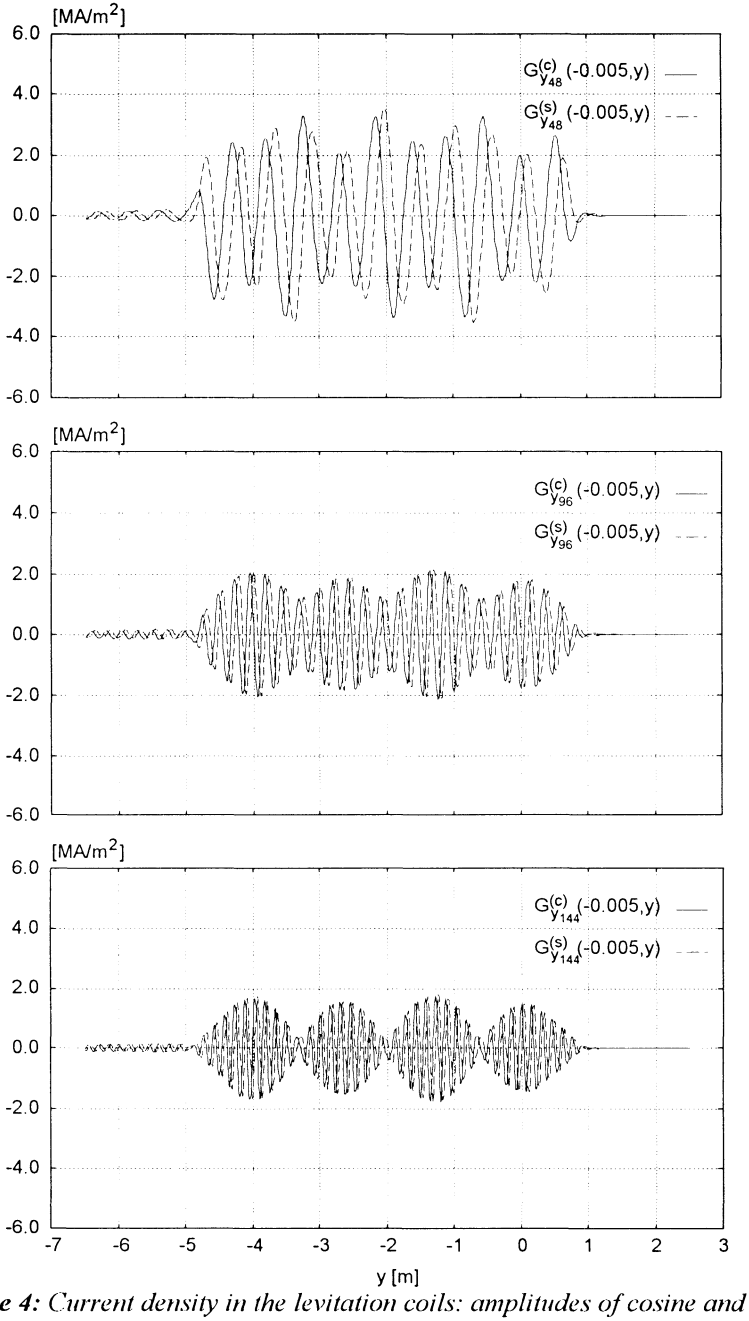

Figure 4: *Current density in the levitation coils: amplitudes of cosine and sine terms of the 1st, 2nd and 3rd harmonic (iN=48, 96, 144) of the y-component along y at x=–0.005 m.*

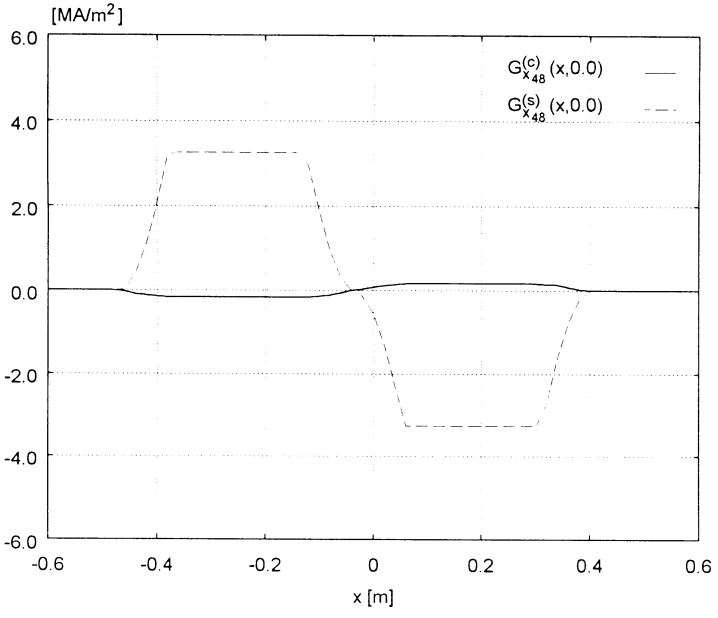

Figure 5: *Current density in the levitation coils: amplitudes of cosine and sine terms of the 1st harmonic of the x-component along x-at y=0.0 m.*

By means of a 2D FEM code, the losses due to the 2nd harmonic have been estimated to be ~20-25% of the losses due to the 1st one. In the following, only the fundamental will be considered, without regarding the analysis as complete.
As regards the distribution along x, $G^{(c)}_{y,iN}$ and $G^{(s)}_{y,iN}$ are different from zero practically only in the levitation coil end-zone; upon a given value of y, the x-distribution of $G^{(c)}_{x,iN}$ and $G^{(s)}_{x,iN}$, is practically trapezoidal (Fig.5).

The problems in the field analysis by means of the 3D FEM code are due both to the limitation on the number of mesh elements (about 30,000, imposed by the available hardware) and to the impossibility to define complicated analytical functions (necessary to describe the distributions of the impressed currents in the levitation coils). Reasonably uncomplicated periodic functions have been then defined in order to approximate (by means of the least squares criterion) the actual distributions of the current density along y.
As the current density distribution is pseudo-periodic and to restrain the number of mesh elements, a longitudinal portion equal to four periods (about 2.15 m) has been considered. The domain of the FEM analysis is then a parallelepiped (2.0 × 2.15 × 2.0 m), symmetrically placed with respect to the current density distribution in the levitation coils (Fig.6). The volume corresponding to the levitation coils has been subdivided into six regions. In the end-zone regions (**1**, **3**, **4** and **6**), analytical functions have been defined in order to represent both the x- and y- component of the current density; in the active length regions (**2** and **5**), only functions representing the x-component have been defined.

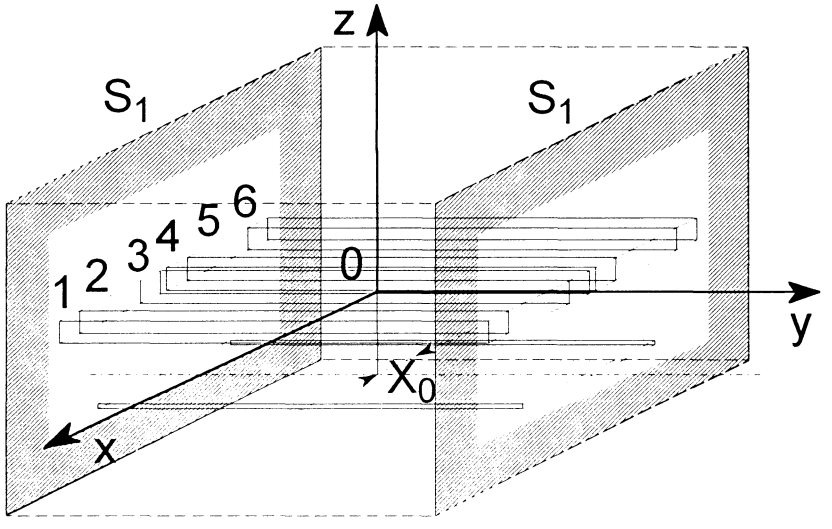

Figure 6: *Domain for the analysis with the 3D FEM code.*

The field contribution of the cosine components has been obtained by means of the following functions:

	$G^{(c)}_{x,48}(x,y)$ [A / m^2]	$G^{(c)}_{y,48}(x,y)$ [A / m^2]
1	$4.095\cdot10^7\cdot(0.4275-x)\cdot\cos[11.7\cdot(y-1.074)]$	$3.5\cdot10^6\cdot\sin[11.7(y-1.074)]$
2	$3.5\cdot10^6\cdot\cos[11.7(y-1.074)]$	0
3	$4.095\cdot10^7\cdot(x-0.0025)\cdot\cos[11.7\cdot(y-1.074)]$	$-3.5\cdot10^6\cdot\sin[11.7(y-1.074)]$
4	$4.095\cdot10^7\cdot(x+0.0025)\cdot\cos[11.7\cdot(y-1.074)]$	$-3.5\cdot10^6\cdot\sin[11.7(y-1.074)]$
5	$-3.5\cdot10^6\cdot\cos[11.7(y-1.074)]$	0
6	$-4.095\cdot10^7\cdot(x+0.4275)\cdot\cos[11.7\cdot(y-1.074)]$	$3.5\cdot10^6\cdot\sin[11.7(y-1.074)]$

Such functions allow to retain the periodicity along y, to verify the condition $\nabla\cdot\overline{\mathbf{G}}=0$ in the whole domain (the boundaries between the regions included) and to fix normal field boundary conditions on the surfaces S_1 of Fig.6 (null field boundary conditions being fixed on the other domain surfaces).
Due to the periodic distribution, the field contribution of the sine components corresponds to the contribution of the cosine components displaced of $\tau/2$ along y and 90° in time. This has been verified by means of 2D analyses. Once the cosine contribution has been calculated, the sine contribution may be calculated by means of a mathematical elaboration; by applying the principle of superposition of effects, the total magnetic field is finally determined.

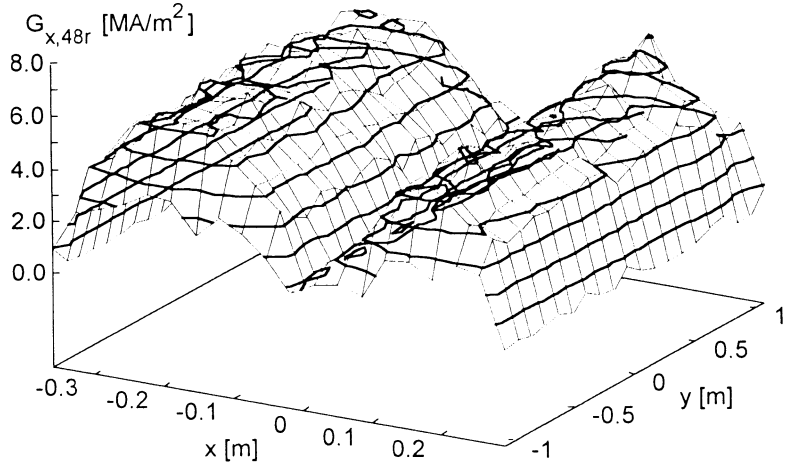

Figure 7: *Amplitude of the fundamental of the x-component* $G_{x,48r}$ *of the current density* $\mathbf{G}_r$ *induced on the surface of the shield.*

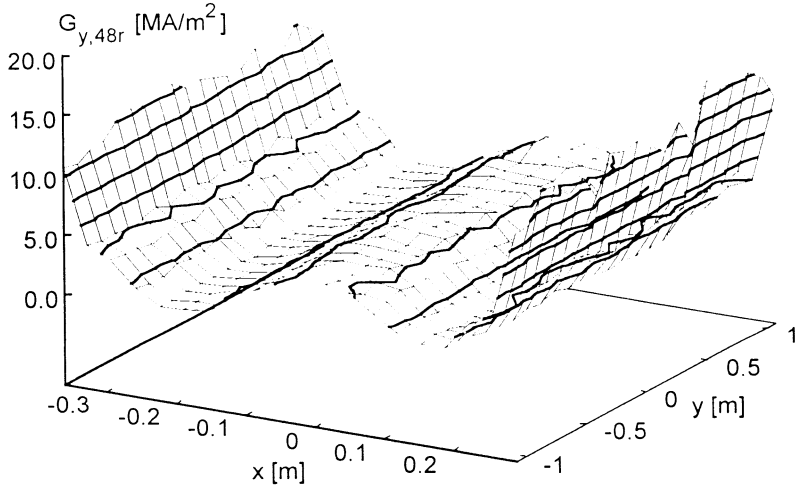

Figure 8: *Amplitude of the fundamental of the y-component* $G_{y,48r}$ *of the current density* $\mathbf{G}_r$ *induced on the surface of the shield.*

The obtained distribution of the eddy current density on the shield surface is given in Figs.7 and 8. The distribution is not very regular, in spite of the periodic functions representing the levitation coil current density: this is due to the domain discretization, mainly. Anyway, the obtained distributions give useful information about the zones where the eddy current density is high. The y-component reaches its peak values on the shield edges which are parallel to the motion direction; such peak values are twice ($1.6 \cdot 10^7$ A/m^2) the ones of the x-component, located on the contrary in front of the regions **2** and **4** of the levitation coils (Fig.7), where the components $G^{(c)}_{x,48}$ and $G^{(s)}_{x,48}$ are higher.

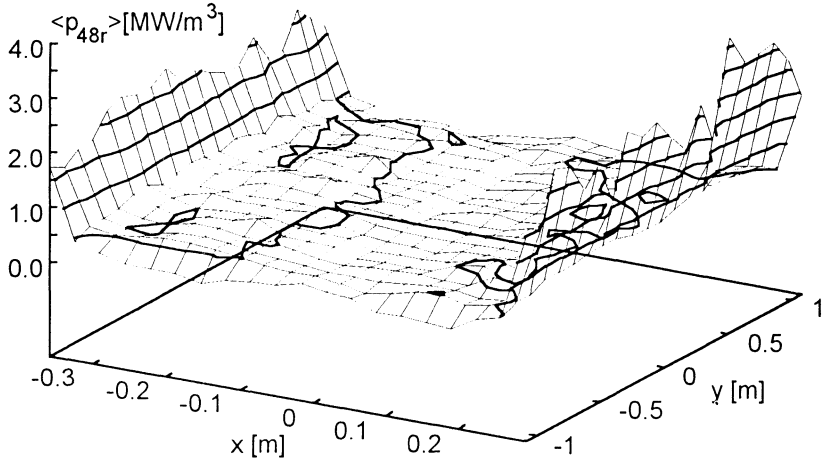

Figure 9: *Power density* $\langle p_{48r} \rangle$ *on the surface of the shield due to the fundamental of the eddy currents.*

As regards the losses, the eddy current distribution causes their concentration in a narrow region on the shield edges (Fig.9): the specific losses reach values higher than $3 \cdot 10^6$ W/m^3 on the shield edge which is in front of the centre of the levitation coils. On the whole, the shield losses per unit length are about 1500 W/m.

6 Conclusions

The paper describes a 3D analytical method to calculate the current density distribution in the on-ground levitation coils of an EDS-MAGLEV train; such distribution is then used as input for a 3D FEM code to determine the eddy currents and the specific losses in the shields of the on-board SC coils.

By analytically representing the current density distribution in the levitation coils with reference to a system fixed to the train, the analysis of the resulting magnetic field may be resolved into the analysis of the field due to the current harmonic components which are time-varying but stationary with respect to the train. In such a way, a 3D FEM code can be utilized, which in itself does not allow to consider dynamical problems.

With reference to a given configuration, the example of application shows the evaluation of the shield eddy currents and losses due to the first harmonic of the current density distribution in the levitation coils.

Appendix

Expressions of coefficients of the Fourier series developed in the main text.

- *Eqn* (1)

$$M_0 = \frac{128\mu_0 N_s N_t}{\pi^2 q_y^5 t_s s_s t_t s_t} \qquad Q'' = q_y \upsilon \frac{L-M}{R} \qquad \varphi_n = 3nq_y b + \arctg(n\lambda_n'' Q'')$$

$$S_n^* = 2\cos(4nq_y b)\sum_{\substack{m=2\ell+1\\ \ell=0,1,2,\ldots}}^{\infty} \mathcal{H}_{nm}\sin\left(mq_x\frac{w}{2}\right)\sin(mq_x X_0)\,e^{-\sqrt{a}Z_0}$$

$$\mathcal{H}_{nm} = \frac{\sin(nq_y b)}{\delta m^2 n^2\sqrt{q}}\sinh\left(\sqrt{q}q_y\frac{s_s}{2}\right)\sinh\left(\sqrt{q}q_y\frac{s_t}{2}\right)\Gamma_{nm}(l_s,h_s,t_s)\Gamma_{nm}(l_t,h_t,t_t)$$

$$b = \frac{l_s + a_y}{2} + t_s \qquad q = n^2 + m^2\delta^2 \qquad a = n^2q_y^2 + m^2q_x^2 = q\cdot q_y^2$$

$$\Gamma_{nm}(l,h,t) = \frac{1}{n-m\delta}\sin\left[(nq_y - mq_x)\frac{t}{2}\right]\cos\left(nq_y\frac{l+t}{2} - mq_x\frac{h+t}{2}\right) -$$
$$-\frac{1}{n+m\delta}\sin\left[(nq_y + mq_x)\frac{t}{2}\right]\cos\left(nq_y\frac{l+t}{2} + mq_x\frac{h+t}{2}\right)$$

- *Eqn* (6)

$$\Gamma_{0m}(l,h,t) = q_y(l+t)\sin\left(mq_x\frac{h+t}{2}\right)\sin\left(mq_x\frac{t}{2}\right) +$$
$$+\left[\frac{2}{m\delta}\sin\left(mq_x\frac{t}{2}\right) - q_y t\cos\left(mq_x\frac{t}{2}\right)\right]\cos\left(mq_x\frac{h+t}{2}\right)$$

- *Eqn* (9)

For i≠0 (considering null the (j–i)th or (i–j)th terms ≤0):

$$G_{x,i}^{(c)}(x,y) = \frac{G_x}{2}\sum_{j=1}^{\infty}\left\{-\gamma_{x,j+i}(x-X_0)\,\iota_j\sin\left[iq_yY_0 - (j+i)q_yy - \varphi_j\right] + \gamma_{x,j-i}(x-X_0)\,\iota_j\cdot\right.$$
$$\left.\cdot\sin\left[iq_yY_0 + (j-i)q_yy + \varphi_j\right] - \gamma_{x,i-j}(x-X_0)\,\iota_j\sin\left[iq_yY_0 - (i-j)q_yy + \varphi_j\right]\right\}$$

$$G_{x,i}^{(s)}(x,y) = \frac{G_x}{2}\sum_{j=1}^{\infty}\left\{\gamma_{x,j+i}(x-X_0)\,\iota_j\cos\left[iq_yY_0 - (j+i)q_yy - \varphi_j\right] - \gamma_{x,j-i}(x-X_0)\,\iota_j\cdot\right.$$
$$\left.\cdot\cos\left[iq_yY_0 + (j-i)q_yy + \varphi_j\right] + \gamma_{x,i-j}(x-X_0)\,\iota_j\cos\left[iq_yY_0 - (i-j)q_yy + \varphi_j\right]\right\}$$

$$G_x = \frac{16N_tM_0I_S}{\pi^2 s_t t_t(L-M)} \qquad \iota_j = \frac{jS_j^*Q''}{\sqrt{1+(j\lambda_j''Q'')^2}}$$

$$\gamma_{x,n}(x-X_0) = \sum_{\substack{m=2k+1\\ k=0,1,2,\ldots}}^{\infty}\frac{\Gamma_{nm}(l_t,h_t,t_t)}{m}\sin\left(mq_x\frac{w}{2}\right)\sin\left[mq_x(x-X_0)\right]$$

For i=0 (synchronous component of G_X, time-invariant with respect to the reference fixed to the vehicle):

$$G_{x,0}^{(c)}(x,y) = \frac{G_x}{2}\sum_{k=1}^{\infty}\gamma_k(x-X_0)\,\iota_k\sin(kq_yy + \varphi_k)$$

- *Eqn* (10)

For i≠0 (considering null the (j–i)th or (i–j)th terms <0):

$$G_{y,i}^{(c)}(x,y) = \frac{G_y}{2}\sum_{j=1}^{\infty}\left\{\gamma_{y,j+i}(x-X_0)\,\iota_j\cos\left[iq_yY_0 - (j+i)q_yy - \varphi_j\right] + \gamma_{y,j-i}(x-X_0)\,\iota_j\cdot\right.$$
$$\left.\cdot\cos\left[iq_yY_0 + (j-i)q_yy + \varphi_j\right] + \gamma_{y,i-j}(x-X_0)\,\iota_j\sin\left[iq_yY_0 - (i-j)q_yy + \varphi_j\right]\right\}$$

$$G_{y,i}^{(s)}(x,y) = \frac{G_y}{2}\sum_{j=1}^{\infty}\left\{\gamma_{y,j+i}(x-X_0)\,\iota_j \sin\left[iq_yY_0-(j+i)q_yy-\varphi_j\right]+\gamma_{y,j-i}(x-X_0)\,\iota_j\cdot\right.$$

$$\left.\cdot\sin\left[iq_yY_0+(j-i)q_yy+\varphi_j\right]+\gamma_{y,i-j}(x-X_0)\,\iota_j\sin\left[iq_yY_0-(i-j)q_yy+\varphi_j\right]\right\}$$

$$G_y = \frac{16N_t\delta M_0 I_S}{\pi^2 s_t t_t (L-M)} \qquad \iota_j = \frac{jS_j^*Q''}{\sqrt{1+(j\lambda_j''Q'')^2}}$$

$$\gamma_{y,n}(x-X_0) = \sum_{\substack{m=2k+1\\k=0,1,2,\ldots}}^{\infty}\frac{\Gamma_{nm}(l_t,h_t,t_t)}{n}\sin\left(mq_x\frac{w}{2}\right)\cos\left[mq_x(x-X_0)\right] \qquad (n\neq 0)$$

$$\gamma_{y,0}(x-X_0) = \sum_{\substack{m=2k+1\\k=0,1,2,\ldots}}^{\infty}\frac{\Gamma_{0m}(l_t,h_t,t_t)}{2m\delta}\sin\left(mq_x\frac{w}{2}\right)\cos\left[mq_x(x-X_0)\right] \qquad (n=0)$$

For i=0 (synchronous component of G_y, time-invariant with respect to the reference fixed to the vehicle):

$$G_{y,0}^{(c)}(x,y) = \frac{G_y}{2}\sum_{k=1}^{\infty}\gamma_{y,k}(x-X_0)\,\iota_k\cos(kq_yy+\varphi_k)$$

List of symbols

Excitation coils

l_s, h_s, s_s, t_s	inner length, inner height and cross section dimensions
N_s, I_s	number of turns and current
a_y	distance between the excitation coils of a bogie
b_y	polar pitch along y (distance between two bogies)

Levitation coils

l_t, h_t, s_t, t_t	inner length, inner height and cross section dimensions of a unit coil
N_t	number of turns of a unit coil
w	vertical distance between the centres of upper and lower unit coil
R, L	resistance and self inductance of a unit coil
M	mutual inductance between upper and lower unit coil
N	number of coils per polar pitch b_y
$p = b_y/N$	pitch

Shield

l_r, h_r, s_r	length, height and thickness
μ, σ	magnetic permeability (equal to μ_0) and electrical conductivity

Relative position between on-board and on-ground coils

X_0	vertical displacement of the vehicle with respect to levitation coils
Y_0+(k-1)p	position along y of the k-th levitation coil at t=0
Z_0	lateral distance between SC and levitation coils
d_{sr}, d_{rt}	distance shield-SC coils and shield-levitation coils

Fourier series expansions [3]

m,n	generic harmonic along x and y, respectively
g_x	fictitious pitch along x

$q_x = \pi/g_x$ $\qquad q_y = 2\pi/b_y$ $\qquad \delta = q_x/q_y$

Acknowledgement

This work was supported by the National Research Council (CNR) under the Progetto Finalizzato "Trasporti 2".

References

1. Murai,T., Fujiwara,S., Characteristics of linear synchronous motor combined propulsion, levitation and guidance, *Int. Conf. on Speedup Technology for Railway and MAGLEV Vehicles,* Yokohama, Japan, November 22÷26, 1993.
2. Saitoh,T. et al. Electromagnetic force and eddy current loss in dynamic behavior of a superconducting magnetically levitated vehicle, *IEEE Trans. on Applied Superconductivity,* vol.3, n.1, March 1993.
3. Andriollo,M., Martinelli,G., Morini,A., Scuttari,A. Calcolo delle correnti indotte negli avvolgimenti di sospensione in sistemi MAGLEV di tipo EDS, *Internal Report UPdie 92-01*, April 1992.
4. Andriollo,M., Martinelli,G., Morini,A. General expressions for forces acting on EDS-MAGLEV systems driven by linear synchronous motors, *Int. Aegean Conf. on Electrical Machines,* Kusadasi, Turkey, May 27÷29, 1992.
5. Andriollo,M., Martinelli,G., Morini,A., Scuttari,A. Mathematical model of on-board power supply for EDS-MAGLEV transport systems, *Symposium on Power Electronics, Electrical Drives, Advanced Electrical Motors,* Taormina, Italy, June 8÷10, 1994